Quaternary Science Reviews 346 (2024) 109085

Contents lists available at ScienceDirect

Quaternary Science Reviews

journal homepage: www.elsevier.com/locate/quascirev

Is the 'Year Without a Summer' imprinted in continental varve thickness records?

Krzysztof Pleskot [a,b,*], Bernd Zolitschka [b]

[a] Geohazards Research Unit, Institute of Geology, Adam Mickiewicz University, Poznań, Krygowskiego 12, 61-680, Poznań, Poland
[b] Institut für Geographie, GEOPOLAR, Universität Bremen, Celsiusstraße 2, 28359, Bremen, Germany

ARTICLE INFO

Handling editor: P Rioual

Keywords:
1815 Tambora eruption
Lake sediments
Varve thickness
Climate event

ABSTRACT

The 1816 CE Year Without a Summer (YWS), following the 1815 CE Tambora eruption, is a classic example of a global cooling event caused by a volcanic eruption. It is well-documented in various historical sources and natural archives. In this study, we investigate whether imprints of this event can be detected in time series of varve and varve sublayer thickness (VT) derived from lake archives. To this end, we examine 43 published and globally distributed VT records covering the period 1766–1866 CE. We hypothesize that thickness anomalies in many VT records correspond to the YWS because it was one of the most prominent climatic events of recent centuries, and VT is a sensitive climate recorder. We evaluate site-specific temperature and precipitation anomalies for the YWS of each investigated lake using available climate model simulations that incorporate proxy and observational data. VT anomalies are identified based on individually selected threshold values for each record, following a robust estimation of trend and variability in the VT data. The climate variables and seasons most influential to VT are determined for each lake based on the related original publications. Our analysis documents that only five records reveal VT anomalies attributable to the YWS. The relationship between VT anomalies and the YWS is questionable in seven records, primarily due to uncertainty about the climatic influence on VT in these cases, and unlikely for the remaining 31 records. The 31 records lacking a YWS signature are divided into two groups. In the first group, the absence of VT anomalies is likely due to weak climate forcing, as temperature and precipitation changed only slightly at those locations. In the second group, while climate forcing was significant, the season during which the anomaly occurred or the specific climate variable that deviated from the long-term mean were not the primary drivers of VT identified in the original studies. We conclude that VT anomalies due to annual climate events are only recorded if a combination of favorable conditions coincides.

1. Introduction

A proper understanding of past climate states is crucial for contextualizing current climate change and indispensable for making climate projections more precise (Tierney et al., 2020). Although increasingly accurate, climate reconstructions still require improvements to limit existing uncertainties and contribute to further advances in paleoclimate research. One avenue proposed to obtain more precise inferences of past climate states is a better understanding of the climate signals in proxy data derived from natural archives (Kaufman and Broadman, 2023).

There are numerous archives that serve as sources of paleoclimatic information, each with their own unique properties. Varved or annually laminated lake sediments are exceptional among these archives in providing precisely dated, annually resolved, and continuous records from the terrestrial realm that extend millennia into the past and cover a wide range of climate variables (Zolitschka et al., 2015). Various approaches were applied to reconstruct climate conditions from varved sediments. Perhaps the simplest yet very efficient approach relies on varve or varve sublayer thickness (VT) measurements. The obtained time series often reveal strong relationships with instrumentally measured climate variables (e.g., Bird et al., 2009; Thomas and Briner, 2009; Vegas-Vilarrúbia et al., 2022). It is this strong relationship that serves as a basis for inferring past climates beyond the coverage of instrumental data.

The correlation between climate parameters and VT results from direct and indirect influences of climate conditions on depositional

* Corresponding author. Geohazards Research Unit, Institute of Geology, Adam Mickiewicz University, Poznań, Krygowskiego 12, 61-680, Poznań, Poland.
E-mail addresses: krzypl@amu.edu.pl (K. Pleskot), zoli@uni-bremen.de (B. Zolitschka).

https://doi.org/10.1016/j.quascirev.2024.109085
Received 29 August 2024; Received in revised form 12 November 2024; Accepted 12 November 2024
Available online 18 November 2024

processes controlling the accumulation of authigenic and allogenic sediment components in lakes. This relationship is site-specific, as lacustrine sedimentation is governed by multiple local factors that modify the original climate signal (Fritz, 2007). Consequently, fluctuations in VT can be explained by different climate variables (e.g., temperature, precipitation, wind speed) and seasons (Zolitschka et al., 2015). Thus, each sedimentary system needs to be understood separately to obtain climatic information properly.

The ability of VT records to infer past climate fluctuations over decades, centuries, and millennia is generally well-established. Therefore, VT records are important components of regional and global climate reconstructions combining information from various paleoclimatic proxies (e.g., Emile-Geay et al., 2017). Much less known, however, is the suitability of VT records to reconstruct annual climate events, perhaps with the exception of climatic extremes associated with major flooding (Schiefer et al., 2007). For the majority of records, it remains to be confirmed whether exceptional short-term temperature or precipitation shifts correspond to anomalous VT. We argue that one way to verify the potential of VT recording short-term climate events is to examine whether existing records of VT anomalies correspond to prominent climate cooling events following major volcanic eruptions (Cooper et al., 2018).

Many volcanic eruptions of the last millennium have significantly influenced global climate, as revealed by comprehensive evaluations based on tree-ring records (Sigl et al., 2015). Cooling episodes, known as volcanic winters, typically last from one to three years and are caused by the formation of sulfuric acid aerosols in the stratosphere that enhance the scattering of incoming solar radiation (Cooper et al., 2018). Among these events, the 1816 CE 'Year Without a Summer' (YWS) associated with the 1815 CE eruption of the Indonesian volcano Tambora is most suitable for examining the potential of VT records to document short-term climate events.

Firstly, the YWS was one of the most severe volcanic winters in history (Sigl et al., 2015) and globally the second coldest year in over 300 years (Neukom et al., 2019), meeting the criterion of prominence. Secondly, the YWS is well-documented in historical documents and proxy data (Brönnimann and Krämer, 2016), allowing for a comprehensive understanding of both the magnitude and geographical extent of related climatic changes. Thirdly, because the event is relatively recent, varve chronologies are expected to suffer only to a minor extent from counting errors, enabling a precise correlation of the event with thickness anomalies. Finally, there is a relatively large number of varve and varve sublayer records from various geographic settings covering the time window of the Tambora event (Ramisch et al., 2020), which facilitates obtaining replicable results.

Although imprints of the YWS on VT records appear reasonable, as many terrestrial land surfaces experienced significant cooling, VT anomalies should not be expected for every record, since the event was not spatially uniform even at regional scales. For instance, the summer of 1816 CE saw a temperature drop of 3 °C below long-term averages in parts of Central and Western Europe, while slight positive temperature anomalies were observed in more eastern parts of the continent (Luterbacher and Pfister, 2015). This spatial heterogeneity in climate is attributed to the varying responses of atmospheric and oceanic circulation to the 1815 CE eruption in different regions, as well as to unforced climate variability, which could either amplify or suppress the effects of volcanic forcing (Raible et al., 2016). Thus, the total contribution of VT records with imprints of the YWS can critically depend on the locations of lakes from which the records have been derived.

In this study, we examine published VT records covering the last ~250 years along with available climate anomaly data for the YWS. Our aim is to identify significant VT anomalies in the records around 1816 CE and evaluate their possible links to the YWS climate event. The obtained results are expected to contribute to a better understanding of the climate signals in VT time series. Given the confirmed sensitivity of VT to climate fluctuations and the prominence of the investigated climate anomaly, we hypothesize that the YWS often correlates with noticeable VT anomalies.

2. Material and methods

We analyze published VT records spanning the 101-year-long period centered at 1816 CE, i.e., the period from 1766 to 1866 CE. Only continuous VT records for the period in focus were included in this study. To obtain relevant data, we searched the following data repositories: (i) VARved sediments DAtabase (VARDA; Ramisch et al., 2020), (ii) World Data Service for Paleoclimatology (WDS-Paleo) at NOAA's National Centers for Environmental Information (Gross et al., 2018), (iii) PANGAEA, the data publisher for Earth and environmental science (Felden et al., 2023), (iv) Geological Society of America (GSA) Data Repository, and (v) Arctic Data Center. Additionally, we performed a literature search for records not available in public data repositories and asked corresponding authors to make their data available for this study. If data of varve sublayer thickness was available, we use it in the analysis instead of total varve thickness values. Sublayers are assigned to two classes: "light layers" and "dark layers". Both are descriptive and include sediments of various composition. For four records, high-quality data was available only for a single class of sublayers. Table 1 lists all 43 records that were examined in this study.

To identify the climate variable and season that mostly influences VT in a given record, we examined the relevant information in the original publications. We described each record, distinguishing positive and negative relationships for one of the four seasons if such a relationship was reported by the authors. We use the designation 'not available' (NA) if the authors provided no information on such a relationship or if the relationship was reported to be weak. Similarly, we use the 'NA' designation if no information is available on the season that influenced VT most or if the relationship with seasons is uncertain.

Climate anomalies for the peak of the YWS (1816 CE) and for the location of lakes were obtained from the global atmospheric paleo-reanalysis dataset EKF400v2, which provides estimates of several climate variables with monthly resolution for the period 1600–2005 CE (Valler et al., 2022). This paleo-reanalysis relies on data assimilation that infers past climate states from both climate model simulations and observational information, i.e., documentary, instrumental, and proxy sources. Precision of the reconstruction can vary depending on the proximity of the grid cell to the nearest observational information and the precision of the information itself. For the period in focus, high density and variability of information are available mainly for Europe and North America, while for most other regions, there is a shortage of information (Valler et al., 2022). This is particularly true for Africa. Based on EKF400v2 data, we investigate the potential climatic effects of the 1815 CE Tambora eruption on both warm and cold seasons in the Northern and Southern Hemispheres. Specifically, we calculated temperature and precipitation anomalies for Northern Hemisphere (NH) summer (June, July, August) of 1816 CE and NH winter (December, January, February) of 1816/1817 CE. The anomalies were calculated with respect to 1766–1866 CE means. We focus on the NH winter of 1816/17 CE instead of 1815/16 CE because for the former noticeably more prominent anomalies were revealed by the paleo-reanalysis.

To identify noticeable anomalies in VT data, we first estimated trends using a running median (*MED*):

$$MED_i = median\{x(i)\}_{i=i-1}^{i+k} \quad (1)$$

where $x(i)$ is the varve thickness at time i, and then calculated time-dependent variability using a running median absolute distance (*MAD*):

$$MAD_i = median\left\{\left|x(j) - median\{x(i)\}_{i=i-k}^{i+k}\right|\right\}_{j=i-k}^{i+k} \quad (2)$$

The smoothing parameter k, which controls the width of the window in calculations, was selected separately for each record from a range

Table 1
List of varved records used in this study with geographical information and references. Column 'ID on map' refers to numbers in Fig. 1. Following Ramisch et al. (2020), we omit the word 'Lake' if it is not an essential part of a lake name, to keep the naming concise.

ID on map	Lake name	Record label	Latitude (°)	Longitude (°)	Country code	Data source	Reference
1	Ayr Lake	Ayr Lake - varve	70.45900	−70.08600	CAN	VARDA	Thomas et al. (2012)
2	Big Round Lake	Big Round Lake - varve	69.86476	−68.85484	CAN	VARDA	Thomas and Briner (2009)
3	Blue Lake	Blue Lake - varve	68.08701	−150.46518	USA	VARDA	Bird et al. (2009)
4	Chala	Chala - light layer	−3.31676	37.70403	KEN	VARDA	Wolff et al. (2011)
5	Chevalier	Chevalier - dark layer	75.05000	−111.50000	CAN	PANGAEA	Amann et al. (2017)
6	Donard	Donard - varve	66.66253	−61.78749	CAN	VARDA	Moore et al. (2001)
7	East Lake	East Lake_1 - varve	74.88821	−109.53417	CAN	VARDA	Cuven et al. (2011)
7	East Lake	East Lake_2 - varve	74.88821	−109.53417	CAN	PANGAEA	Lapointe et al. (2017)
8	Elk Lake	Elk Lake - varve	47.18905	−95.21790	USA	VARDA	Dean and Megard (1993)
9	Etoliko	Etoliko - light layer	38.47323	21.32478	GRC	VARDA	Koutsodendris et al. (2017)
9	Etoliko	Etoliko - dark layer	38.47323	21.32478	GRC	VARDA	Koutsodendris et al. (2017)
10	Green Lake	Green Lake - varve	50.20000	−122.90000	CAN	WDS-Paleo	Schiefer et al. (2007)
11	Holzmaar	Holzmaar - varve	50.11889	6.87917	DEU	Author	Zolitschka (1996)
12	Hvítárvatn	Hvítárvatn_1 - varve	64.61014	−19.84015	ISL	VARDA	Larsen et al. (2011)
12	Hvítárvatn	Hvítárvatn_2 - varve	64.61014	−19.84015	ISL	VARDA	Larsen et al. (2011)
13	Iceberg Lake	Iceberg Lake_1 - varve	60.78804	−142.95885	USA	VARDA	Loso (2009)
13	Iceberg Lake	Iceberg Lake_2 - varve	60.78804	−142.95885	USA	VARDA	Diedrich and Loso (2012)
14	Kassjön	Kassjön - varve	63.92566	20.00977	SWE	Author	Arnqvist et al. (2016)
15	Kenai	Kenai - varve	60.38806	−149.6011	USA	GSA	Boes et al. (2017)
16	Kuninkaisen-lampi	Kuninkaisen-lampi - light layer	63.98333	28.02333	FIN	Author	Saarni et al. (2016)
16	Kuninkaisen- lampi	Kuninkaisen- lampi - dark layer	63.98333	28.02333	FIN	Author	Saarni et al. (2016)
17	Kusai	Kusai - light layer	35.69167	92.83333	CHN	Author	Zhang et al. (2022)
17	Kusai	Kusai - dark layer	35.69167	92.83333	CHN	Author	Zhang et al. (2022)
18	Lake C2	C2 Lake - varve	82.82759	−77.98599	CAN	VARDA	Lamoureux and Bradley (1996)
19	Lake DV09	DV09 Lake - varve	75.57439	−89.30943	CAN	VARDA	Courtney Mustaphi and Gajewski (2013)
20	Lehmilampi	Lehmilampi - varve	63.62829	29.10224	FIN	VARDA	Haltia-Hovi et al. (2007)
21	Linnévatnet	Linnévatnet - varve	78.04472	13.807222	NOR	ADC	Lapointe et al. (2023)
22	Lower Murray Lake	Lower Murray Lake - varve	81.33275	−69.55102	CAN	VARDA	Cook et al. (2009)
23	Montcortès	Montcortès - light layer	42.33158	0.99491	ESP	PANGAEA	Vegas-Vilarrúbia et al. (2022)
24	Nar Gölü	Nar Gölü - light layer	38.34037	34.45611	TUR	Author	Roberts et al. (2019)
24	Nar Gölü	Nar Gölü - dark layer	38.34037	34.45611	TUR	Author	Roberts et al. (2019)
25	Nautajärvi	Nautajärvi - light layer	61.80000	24.68330	FIN	WDS-Paleo	Ojala and Alenius (2005)
25	Nautajärvi	Nautajärvi - dark layer	61.80000	24.68330	FIN	WDS-Paleo	Ojala and Alenius (2005)
26	Oeschinen	Oeschinen - varve	46.49841	7.72744	CHE	VARDA	Amann et al. (2015)
27	Ogac	Ogac - light layer	62.84316	−67.34011	CAN	VARDA	Hughen (2009)
27	Ogac	Ogac - dark layer	62.84316	−67.34011	CAN	VARDA	Hughen (2009)
28	Plomo	Plomo - varve	−47.00475	−72.91217	CHL	VARDA	Elbert et al. (2015)
29	Sawtooth	Sawtooth - varve	79.34939	−83.92353	CAN	VARDA	Francus et al. (2002)
30	Skilak	Skilak_1 - varve	60.40198	150.30434	USA	GSA	Boes et al. (2017)
30	Skilak	Skilak_2 - varve	60.40198	150.30434	USA	GSA	Boes et al. (2017)
31	Upper Sopper	Upper Sopper - dark layer	62.91667	−69.53000	CAN	WDS-Paleo	Hughen et al. (2000)
32	Żabińskie	Żabińskie - light layer	54.13180	21.98360	POL	Author	Żarczynski et al. (2019)
32	Żabińskie	Żabińskie - dark layer	54.13180	21.98360	POL	Author	Żarczynski et al. (2019)

between 6 and 14 to minimize the cross-validation criterion C_1 presented by Zheng and Yang (1998):

$$C_1 = \frac{1}{n}\sum_{i=1}^{n}\left|x(i) - median\{x(j)\}_{j=i-k}^{i+k}\right| \quad (3)$$

Limiting k to the range $[6, 14]$, which results in a window width of 13–29 years (window width $= 2k + 1$), aims to avoid solutions that use either very large or very small k values. If no pre-selection is made, an erroneous k can be suggested by the C_1 criterion, as it is not completely immune to autocorrelation typically occurring in time series (Mudelsee, 2014). We used *MED* and *MAD* because these are robust estimators not biased by extremes. Since methods relying on moving windows truncate the original records at both ends, we used records longer than 101 years as input. This approach eliminated the need to extrapolate the resulting records to obtain *MED* and *MAD* values for the entire time range of 1766–1866 CE. Following Besonen et al. (2008), we consider the thickness of a layer to be anomalously large or small if it exceeds the threshold detection value (*TDV*) defined by:

$$TDV = MED + MAD \times z \quad (4)$$

To identify solutions where anomalies constitute no more than 5% of all observations, we examined various values of the scalar z. For positive anomalies, we tested z values of 2, 3.5, and 5, while for negative anomalies, we used values of 1, 1.75, and 2.5. Lower z values were examined to detect negative extremes, considering the hard boundary at 0 mm. The final decision on selecting z for positive and negative anomalies was based on evaluating the number of identified anomalies. For VT that exceeded upper or lower thresholds, we calculated the magnitude of the anomaly (S_m) considering the sample-specific *MAD*:

$$S_m = \frac{x(i) - MED}{MAD} \quad (5)$$

As a first approximation, we consider an anomaly to be potentially related to the YWS if it occurred at 1816 ± 7 CE. We applied the same chronological uncertainty level to all records because, in most cases, chronological uncertainty was not evaluated. The ±7-year range corresponds to a chronological uncertainty of 3.5% relative to the YWS. This slightly exceeds the ±2% suggested by Ojala et al. (2012) as a realistic error for most varve chronologies. However, we decided to use a relatively long-time window to avoid excluding anomalies around the YWS that may arise from records potentially suffering from lower chronological precision.

To evaluate the site-specific relationship between VT and climate variables, independent of the information provided by original publications, we ran correlations between climate data extracted from the relevant grids of EKF400v2 spanning the reference period of 1766–1866 CE and the VT records. Correlation coefficients were calculated using annual summer and winter averages of temperature and precipitation,

as well as detrended VT time series. The detrended VT value $x_d(i)$ was calculated as:

$$x_d(i) = x(i) - MED \quad (6)$$

A Spearman's rank correlation coefficient (ρ) was calculated instead of Pearson's linear correlation coefficient (r) due to the asymmetric distribution of VT data. To account for possible time lags in the VT response to climate variations and the chronological imprecision of the VT records, we tested solutions with lags ranging from −10 to +10 years for selecting the highest ρ for each season, each climate variable, and the VT record individually.

3. Results

3.1. Distribution of lakes with varved sediments and YWS climate anomalies at their respective locations

The records examined come from 32 lakes (Table 1). Most are located in North America (n = 17) and Europe (n = 11), while two are from Asia and one each from Africa and South America (Fig. 1). Temperatures during the NH summer of 1816 CE were noticeably lower than average for the period 1766 to 1866 CE for most of the Earth's land surface. There is a cooling reported for most of the lake locations, with the most prominent deviation from the reference period found at Oeschinen, in the Swiss Alps (2.7 °C colder than the 1766–1866 CE average). Slight warming was detected at only eight sites. During the NH winter of 1816/1817 CE, large parts of eastern North America were noticeably colder than usual, while Europe and western Asia were warmer than average. Temperature changes in other regions were comparatively small. Accordingly, the most pronounced cooling was found at lakes located in Arctic Canada, reaching a minimum at Ogac (6 °C colder than the 1766–1866 CE average; Fig. 2), whereas positive anomalies were mostly reported for European sites, with a maximum at Żabińskie, Poland (temperatures 3.3 °C higher with respect to the reference period).

Spatial manifestation of precipitation anomalies for the NH summer 1816 CE is less uniform compared to temperature anomalies (Fig. 1). We found that slightly more than half of the sites (n = 18) experienced less precipitation than the 1766–1866 CE average. Departures from the mean were mostly small (<25%) but at Nar Gölü in Turkey (no. 24 in Fig. 1), there was more than twice as much precipitation as expected from the long-term mean (217%, Fig. 2). During the NH winter of 1816/1817 CE, precipitation anomalies also varied spatially. For most of the locations (n = 26) it was drier than average with a minimum of 62% of the average reported for Donard in Canada (no. 6 in Fig. 1). The only site with a noticeable positive anomaly is Kusai on the Tibetan Plateau (China; 127%; no. 17 in Fig. 1).

3.2. Characteristics of VT time series

Of the studied records, 25 provide total varve thickness measurements, and together 18 light and dark sublayer thickness measurements. According to information provided by the original publications, 28 records reveal a clear association with a climate variable (Fig. 3). Of these, only two records revealed a negative relationship with the driving climate variable, whereas the remaining records show a positive relationship. The most common climate-related variable influencing VT is temperature (n = 17), followed by precipitation (n = 5), hydrological extremes (n = 5), and wind strength (n = 1). Although for most records (n = 19) summer is the most important season controlling VT, some records reveal associations with other seasons (three with winter, two with spring, and one with autumn). In the case of three records revealing relationships with a climate variable, none of the seasons played a dominant role.

The records differ markedly in terms of their maximum amplitude of fluctuations, average thicknesses, and overall variability (Fig. 4). In the records from Kuninkaisenlampi (Finland), the VT between 1785 and 1794 CE is derived from interpolation (shown as red shading in Fig. 4). Therefore, we excluded this interval from further analyses. Altogether, we found four VT values that equal zero. Excluding these values, the minima of VT range from 0.001 to 3.35 mm. Even more pronounced differences were determined for median thicknesses (ranging from 0.031 to 8.91 mm), and for maximum thicknesses (ranging from 0.091 to 34.29 mm). The noticeable difference in variability of thicknesses is evident from the wide range of standard deviation (0.02–5.31 mm).

3.3. Correlations between EKF400v2 climate time series and VT records

The calculated correlations between seasonal averages of climate variables and the detrended VT time series were low for each variable in each record, with a maximum $\rho < 0.4$, even when considering the most favorable lags (Supplementary Information, Fig. S1). We assume that this result is primarily due to the coarse spatial resolution of EKF400v2, which is inadequate for evaluating the site-specific relationship between VT and climate variables. Consequently, we abandoned further exploration to determine which climate variable and season are most important for controlling VT in the investigated records using EKF400v2. Instead, we rely on the information provided by the original publications.

3.4. VT outlier detection

The criterion we used to select the optimal smoothing factor k in calculating *MED* (Eq. (1)) and *MAD* (Eq. (2)) yields variable results ranging from minimum (6) to maximum (14) pre-selected values of k. Accordingly, window sizes used in calculations vary from 13 to 29 (specific window sizes used are provided in parentheses next to the site names in Fig. 4). We observed noticeable differences in the number of outliers detected depending on the selection of the z value for Eq. (4) (Fig. 5). The median number of negative outliers for various z values are: 19 ($z = 1$), 7 ($z = 1.75$) and 2 ($z = 2.5$). Similarly, for positive anomalies, the median number of detected outliers varies from 14 ($z = 2$) through 6 ($z = 3.5$) to 3 ($z = 5$). The solution closest to the desired outcome, with the majority of records containing not more than 5% anomalous observations, was achieved with $z = 2.5$ for negative and $z = 5$ for positive extremes.

In the selected solution, the total number of identified outliers varies from 1 to 14. For 17 records, there was no negative anomaly, whereas a positive anomaly was absent in only two records. The maximum number for negative and positive anomalies are 10 and 14, respectively. Within the time range 1816 ± 7 CE, no anomalies were found for 18 records, a single anomaly was found for 15 records, and more than one anomaly was identified for 10 records (Fig. 6). For Ayr Lake - varve, Chala - light layer, Donard - varve, Green Lake - varve, Holzmaar - varve, Iceberg Lake_1 - varve, Nar Gölü - light layer, Nautajärvi - dark layer, Oeschinen - varve, and Żabińskie - dark layer, we conclude that the scaled magnitude of the anomaly at 1816 ± 7 CE is exceptional compared to the remaining anomalies (Fig. 6).

4. Discussion

4.1. Spatial patterns of climate anomalies during the YWS and their drivers

Although it appears obvious that climate conditions in 1816 CE differed noticeably from long-term averages, there remain uncertainties regarding the amplitude of changes in temperature and precipitation as well as their spatial variability (Raible et al., 2016). Therefore, before discussing the relationship between VT and climate anomalies of the YWS, we provide an overview of the EKF400v2 output for the period in focus to examine how it corresponds to the current understanding of the climatic impacts after the Tambora eruption in 1815 CE.

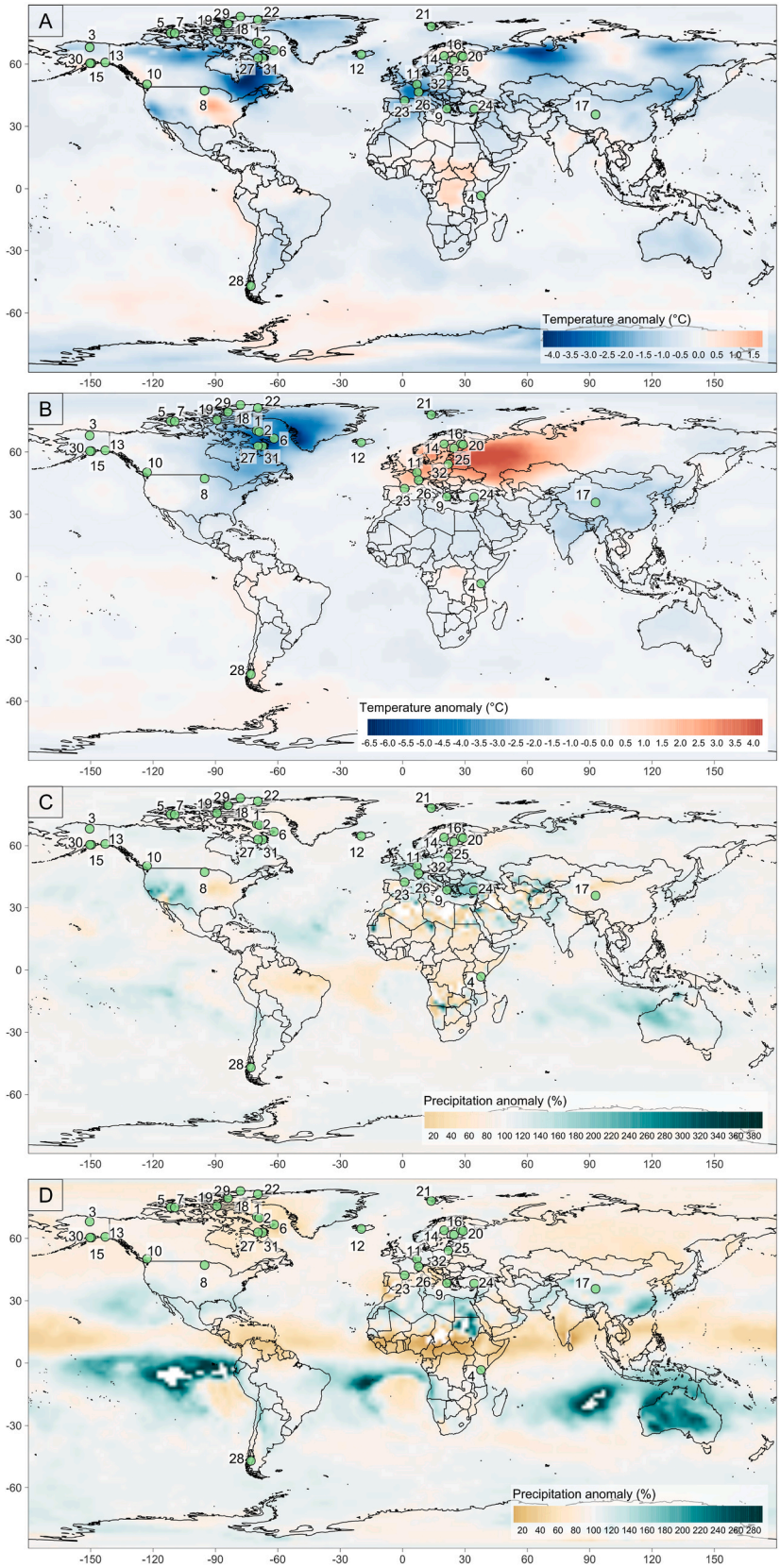

Fig. 1. Maps showing temperature and precipitation anomalies during the 'Year Without a Summer' of 1816 relative to the 1766–1866 mean. (A) Northern Hemisphere (NH) summer (June, July, August) temperatures in 1816 CE, (B) NH winter (December, January, February) temperatures in 1816/1817 CE, (C) NH summer precipitation in 1816 CE, and (D) NH winter precipitation in 1816/1817 CE. Precipitation anomalies are expressed as deviations from the mean in percentages, with 100% corresponding to no change. Data are from the EKF400v2 reconstruction (Valler et al., 2022). Locations of investigated lakes are marked with dots and their ID numbers (Table 1).

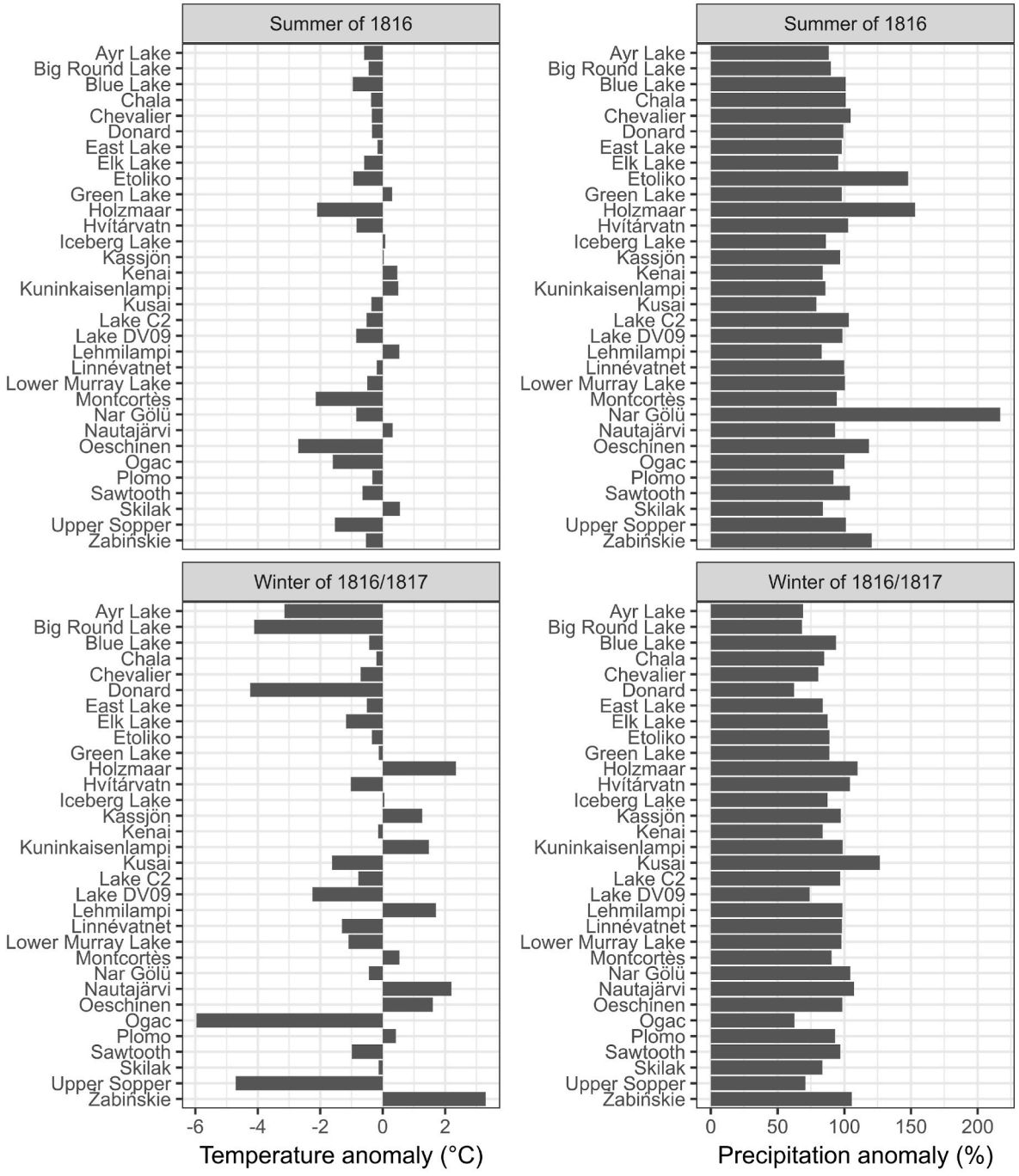

Fig. 2. Climate anomalies at the investigated lake sites for Northern Hemisphere summer (June, July, August) of 1816 CE and winter (December, January, February) of 1816/1817 CE. The estimates are derived from EKF400v2 (Valler et al., 2022). Temperature anomalies are reported as deviations from their means of the 1766–1866 CE reference period, whereas precipitation anomalies are expressed as deviations from the mean for the same reference period, with 100% corresponding to no change.

Perhaps the most well-documented pattern of temperature change related to the YWS concerns the notable cooling of Western Europe and parts of Eastern North America, accompanied by little to no temperature change or slight warming in Eastern Europe and other parts of North America (Luterbacher and Pfister, 2015; Raible et al., 2016). This pattern, which can be largely attributed to unforced climate variability (Brönnimann and Krämer, 2016), possibly was related to an unusual Rossby-wave configuration (Raible et al., 2016) and is well reproduced by EKF400v2 (Fig. 1A). The paleo-reanalysis also agrees with previous studies, showing limited cooling in the Southern Hemisphere during the summer of 1816 CE. Raible et al. (2016) explain this by negligible effects of the Tambora eruption on two primary modes of internal climate variability influencing the Southern Hemisphere: the El Niño/Southern Oscillation and the Southern Annular Mode.

In the winter of 1816/17 CE, cooling in Northeastern North America and warming in Central and Eastern Europe are the only notable temperature changes suggested by EKF400v2 (Fig. 1B). This pattern of temperature anomalies revealed by paleo-reanalysis for the North Atlantic region was already reported in previous studies (Fischer et al., 2007; Ortega et al., 2015) and can be expected during a positive phase of the North Atlantic Oscillation (NAO; Ortega et al., 2015). It remains likely that the Tambora eruption contributed to the switch to a positive

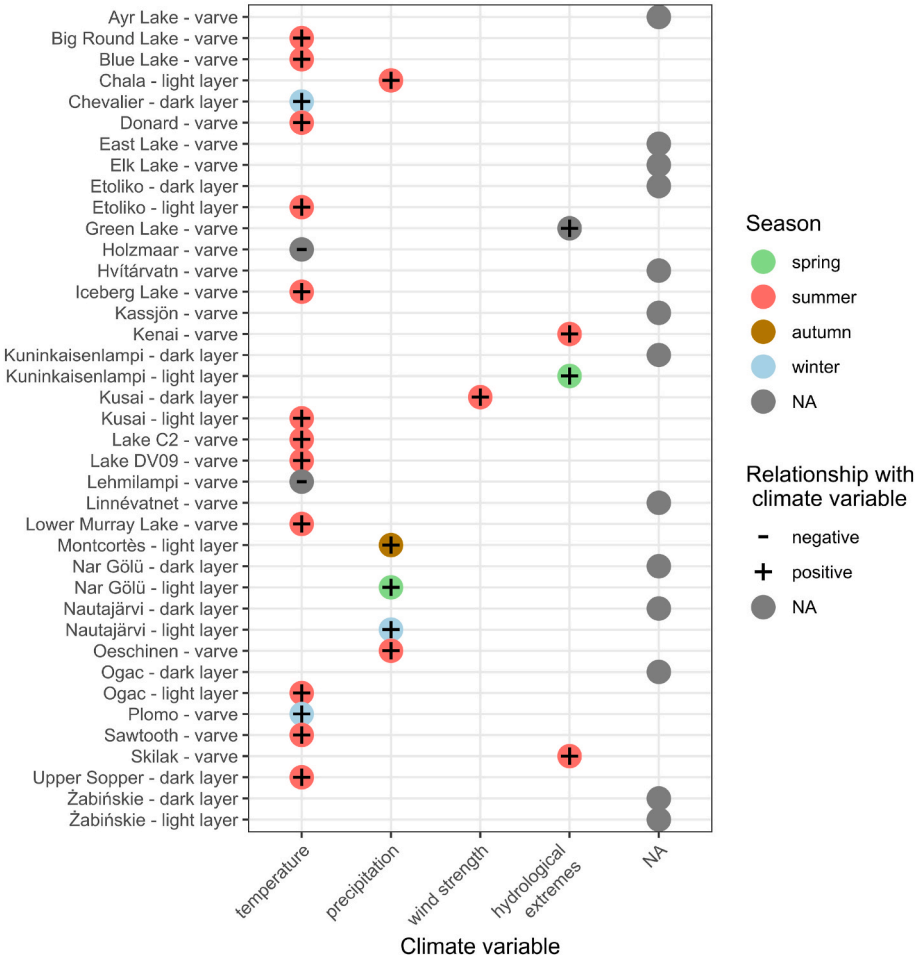

Fig. 3. Relationship between varve and varve sub-layer thicknesses (VT) and climate-related variables. Relationships are identified based on information provided by original publications (see Table 1 for references). Note that for all records, including those from the Southern Hemisphere, the identification of seasonal affinity relies on Northern Hemisphere seasons to facilitate cross-referencing with Figs. 1 and 2. NA – not available.

NAO phase through intensification of the polar vortex (Trigo et al., 2009; Wang et al., 2023), even though this is not well reproducible by some climate models (Raible et al., 2016).

EKF400v2 successfully reproduces negative anomalies in precipitation over monsoon regions of Africa, East Asia, and North America for the summer of 1816 CE (Fig. 1C), previously recognized in climate model simulations (Brönnimann and Krämer, 2016). A decrease in precipitation following large tropical volcanic eruptions is expected due to the weakening of monsoon circulation. This weakening occurs because land surfaces cool more rapidly than oceans in response to increased scattering of solar radiation in the stratosphere caused by volcanic sulfur aerosols. The resulting change in the temperature gradient between land and ocean disrupts the monsoon system, leading to reduced rainfall. Positive anomalies in summer precipitation over Central Europe, which have been explained by a weakening and expansion of the Hadley Cell following the Tambora eruption (Wegmann et al., 2014) are also evident in the map derived from EKF400v2 (Fig. 1C).

Precipitation anomalies reconstructed by EKF400v2 for the winter of 1816/17 CE support a positive NAO phase inferred from temperature patterns by showing drying in Southern Europe and Northern North America and wetting in Southern North America (Fig. 1D). Moister conditions of Northern Europe expected during a positive winter NAO phase is less evident. In addition to anomalies at high latitudes, EKF400v2 also shows noticeable changes in winter precipitation for the tropics, which could have been associated with a migration of the Intertropical Convergence Zone in response to the eruption (Iles et al., 2013).

In summary, the patterns of temperature and precipitation changes reconstructed from EKF400v2 for the summer of 1816 CE and the winter of 1816/17 CE align with the current understanding of climate anomalies following the Tambora eruption. Therefore, the reanalysis output appears suitable for examining the relationship between climatic effects of the eruption and VT records. Nonetheless, the anomalies extracted from EKF400v2 for the lake sites investigated in this study only approximate the true anomalies, as lakes certainly respond to more local climate variations that can differ largely from anomalies averaged over $2 \times 2^{\circ}$ grid cells. Thus, caution is needed when interpreting the results.

4.2. *Relationship between VT anomalies and the YWS*

Understanding the relationships between VT anomalies and climate perturbations following the 1815 CE Tambora eruption is a challenging task. With no direct proxy currently available for identifying this volcanic event in the records, we rely on correlating changes in VT along calendar year-dated but imperfect time series. Despite this difficulty, we argue that it should be possible to assess the likelihood of a YWS imprint on lacustrine VT records by relying on our robust identification of VT anomalies (Fig. 6). Furthermore, combining knowledge of site-specific relationships between climate and VT (Fig. 3) and the available and up-to-date understanding of climate anomalies during the YWS (Fig. 2) is helpful. Accordingly, we distinguish four categories of records that

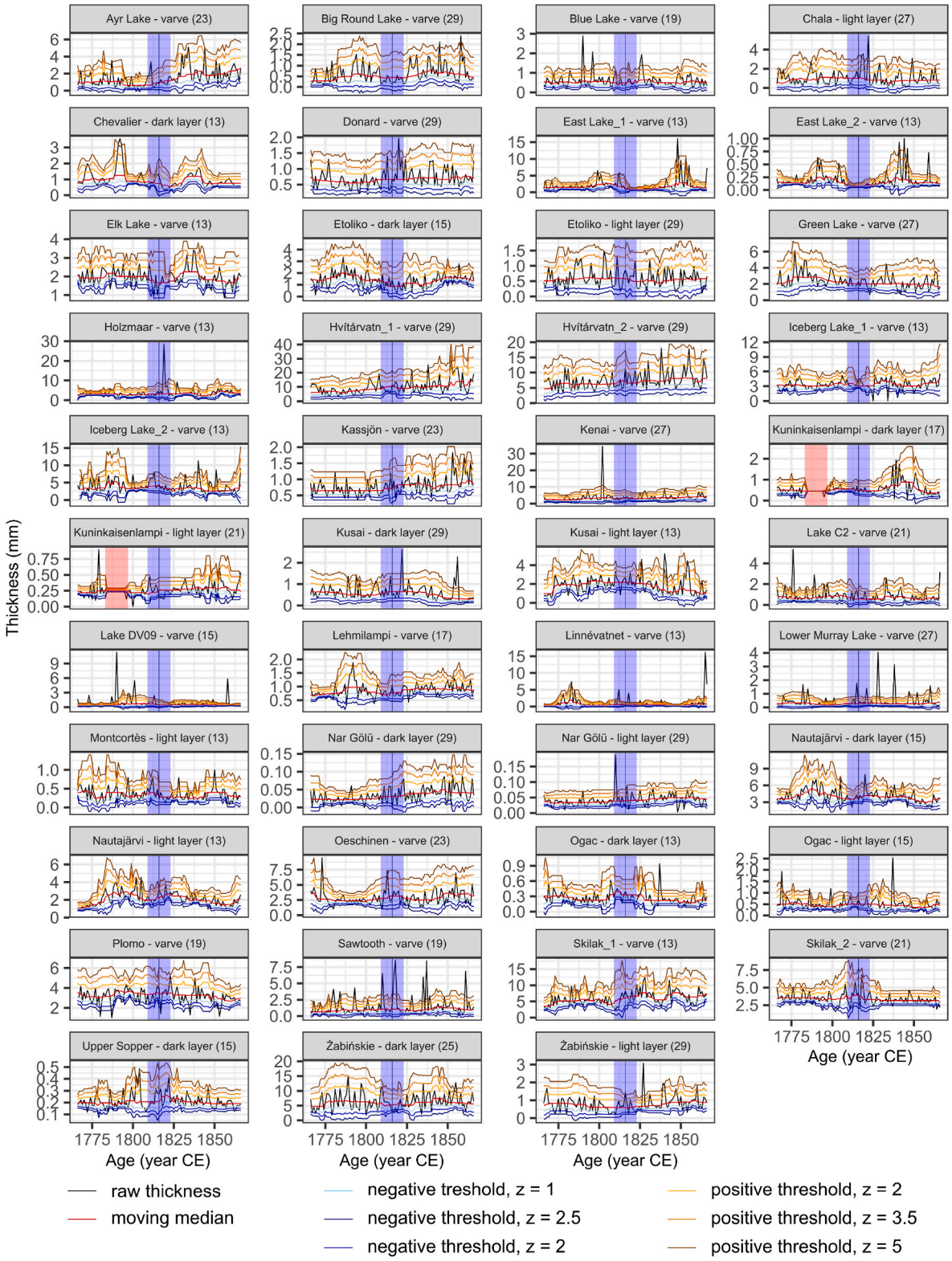

Fig. 4. Varve and varve sub-layer thickness (VT) time series with various thresholds for differentiating thickness anomalies. Sample-specific negative and positive threshold detection values were estimated considering various z values (see Eq. (4)). Red shading documents the range of VT data from Kuninkaisenlampi excluded from analysis due to interpolation. Numbers in parentheses show the width of the window used for calculations.

differ in their potential to contain an imprint of the YWS (Fig. 6): (i) YWS imprint unlikely A; (ii) YWS imprint unlikely B; (iii) YWS imprint questionable; and (iv) YWS imprint likely. Below, we characterize each category and explain in detail how the categorization was performed.

4.2.1. *YWS imprint unlikely A*

This category comprises all 18 records where no anomalies were detected within the time range of 1816 ± 7 CE years (Fig. 6). For the majority of records in this category, the absence of anomalies can likely be attributed to a small magnitude of the climate anomaly or site-

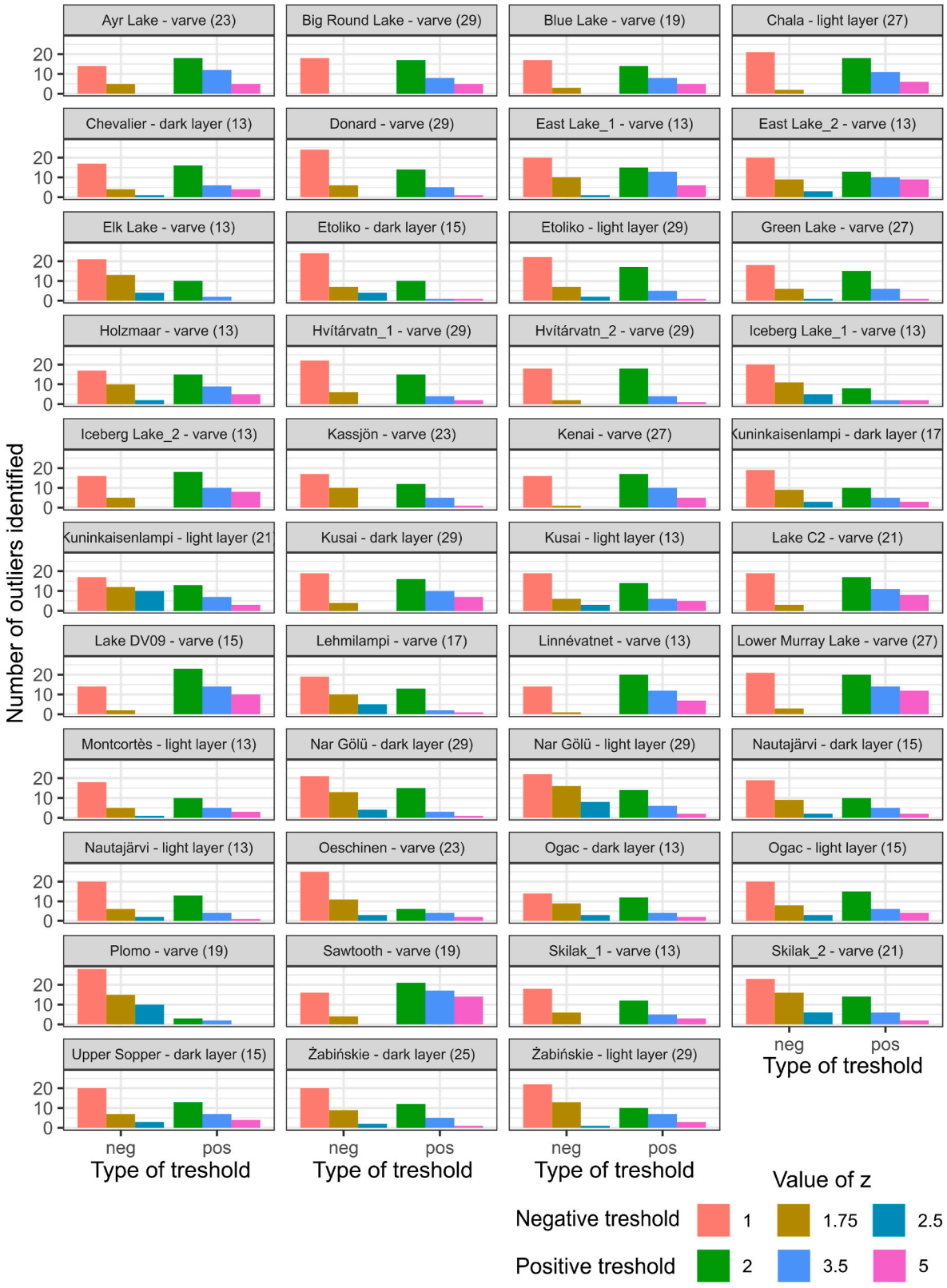

Fig. 5. Number of identified outliers of varve and varve sub-layer thickness (VT) time series for various selections of the z value (Eq. (4)). Final results rely on the solution with z = 2.5 for identification of negative anomalies and z = 5 for identification of positive anomalies.

specific relationships between varve-formation processes and climate. For example, according to EKF400v2, precipitation during the YWS was close to the long-term average, and temperature change did not significantly exceed 1 °C for the locations of Blue Lake, Chevalier, Elk Lake, Hvítárvatn, Kassjön, Kenai, Lake C2, Skilak (Fig. 2). Although the climate influence was more distinct for Big Round Lake - varve, Etoliko - light layer, Lehmilampi - varve, Montcortès - light layer, Nautajärvi - light layer, and Nar Gölü - dark layer, either the climate variable or the

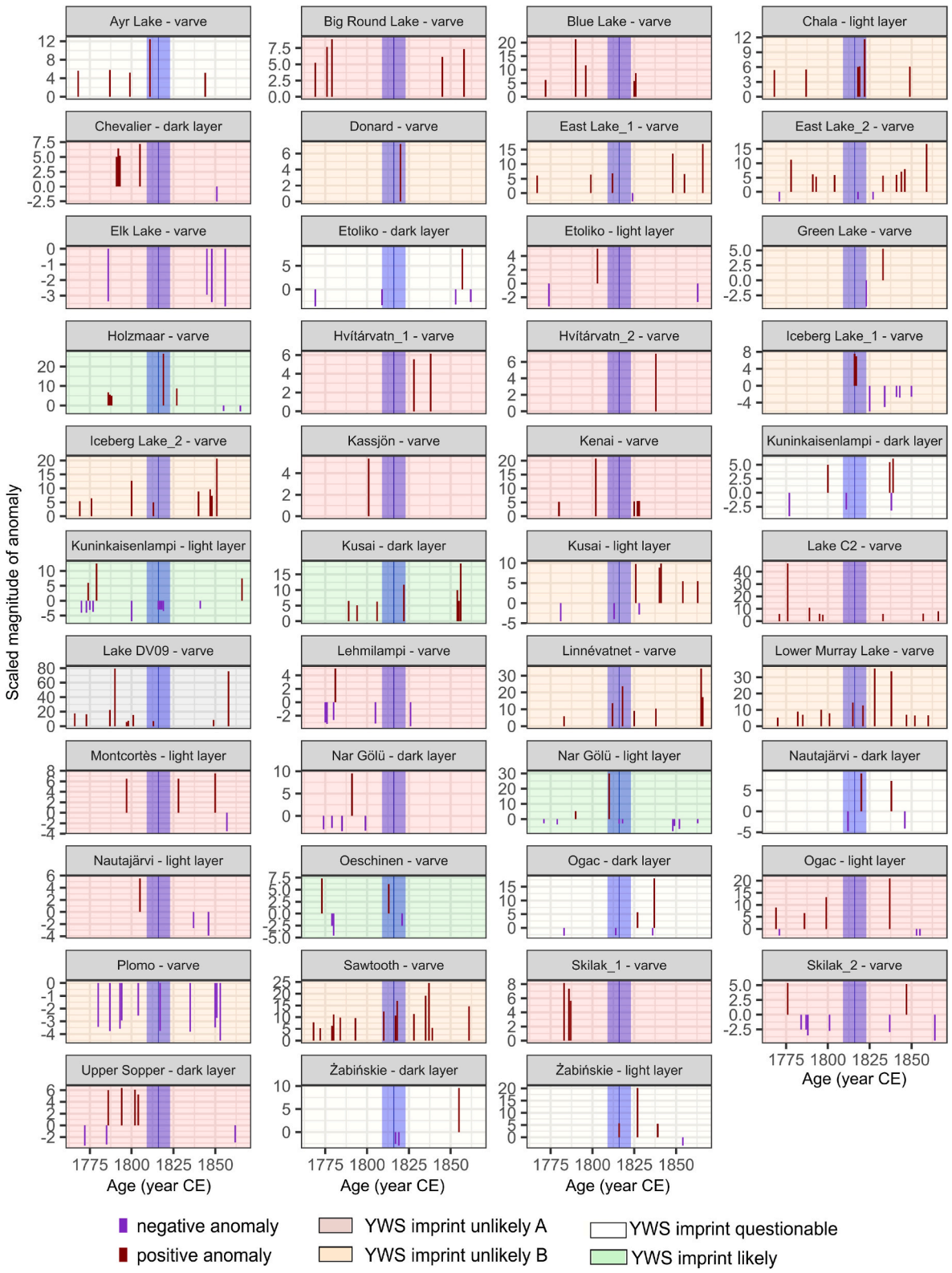

Fig. 6. Scaled magnitude anomalies in varve and varve sub-layer thickness (VT) time series. Anomalies are identified based on the solution with z = 2.5 for negative anomalies and z = 5 for positive anomalies (cf. Eq. (4)). The background color of the plots refers to the likelihood of the presence of a YWS imprint in the records. Description of how the categorization was carried out is provided in the text of chapter 4. The year 1816 CE is marked by a vertical black line, and the shading around this line represents the range of 1816 ± 7 years CE.

season, during which the anomaly occurred, was not attributed as having a dominant influence on VT in the original publications (Figs. 2 and 3).

There are only two records in the first category where an anomaly was expected but not observed: Ogac - light layer and Upper Sopper - dark layer. For both cases, summer temperatures, which are the most significant predictors of VT (Fig. 3), declined more than 1.5 °C (Fig. 2). One possible explanation for the lack of a significant thickness anomaly in these records is that Ogac and Upper Sopper are located in Arctic Canada, a region likely characterized by exceptionally large year-to-year temperature fluctuations (Olonscheck et al., 2021). Therefore, despite a temperature change of 1.5 °C noticeable on a global scale, it was likely insignificant locally.

4.2.2. YWS imprint unlikely B

In this category, there are thirteen records showing anomalies in the period 1816 ± 7 CE that should not be present if the climate shift during the YWS was the main driver controlling VT and if the VT-climate relationship was correctly identified in the original publications (Fig. 6). During the YWS, summer temperatures were slightly lower for locations of the following records: Donard - varve, DV09 - varve, Lower Murray Lake - varve, and Sawtooth - varve (Fig. 2). Since these records show a positive relationship with summer temperature (Fig. 3), a negative anomaly, if any, has to be expected. However, in each case, a positive anomaly is present. For the remaining records in this category, namely East Lake_1 - varve, East Lake_2 - varve, Green Lake - varve, Iceberg Lake_1 - varve, Iceberg Lake_2 - varve, Kusai - light layer, Linnévatnet – varve, Plomo - varve, and Chala - light layer, climate anomalies relevant to the thicknesses were all minimal (Fig. 2) and thus should not be considered as sole explanatory factors for exceptionally thick or thin layers.

We separated this category from 'YWS unlikely A' because we cannot completely exclude the possibility that there may exist more complex relationships between the YWS and VT, or that climate anomalies not considered as important may have influenced these records. For instance, here we considered only seasonal averages, which, despite providing an important first-order approximation of past climate conditions, are not able to capture the entire climate variability that might have influenced lacustrine sedimentation. Also, it is possible that the relationship between climate variables and the thickness has changed over time. This was reported for the record from Lake Silvaplana, Switzerland, which revealed a positive relationship with temperature over the 20th and a negative relationship in the 19th century (Blass et al., 2007). However, any discussion of potential influences of factors that cannot be reliably reconstructed would inevitably remain speculative. Therefore, we argue that given the available data, it appears reasonable to consider the imprint of the YWS in records of the second category as unlikely.

Perhaps the most interesting record in the second category is Chala - light layer (Kenya), where one of the three anomalies found at 1816 ± 7 CE was exceptionally large, even if considered on a multi-millennial timescale (Wolff et al., 2011). Yet, NH summer precipitation, which is the strongest predictor of thicknesses in this case (Fig. 3), remained unchanged during the YWS (Fig. 2). One argument could be that the EKF400v2 climate reconstruction for Lake Chala is not very precise due to the large distance to the nearest instrumental weather station or any proxy record (Valler et al., 2022). However, another line of evidence suggests that precipitation has not markedly changed during the YWS. Precipitation in central-east Africa is driven to a large extent by ENSO oscillations with particularly wet NH summers corresponding to prominent La Niña events (Wolff et al., 2011). Thus, any anomalously wet summers should be traceable in the ENSO index record, which apparently does not show any noticeable shifts around 1816 CE (Li et al., 2013). Therefore, we assume that EKF400v2 is probably not exceedingly wrong in suggesting no noticeable NH summer precipitation anomaly for 1816 CE in East Africa. Consequently, the prominent anomaly in the Chala - light layer record is most likely driven by processes not directly related to the climate impacts of the 1815 CE Tambora eruption and its presence around 1816 CE is a coincidence.

4.2.3. YWS imprint questionable

Seven records fall into the third category and reveal a complex relationship with climate, without any single variable dominating the influence on VT (Fig. 3). Although this complex relationship prevents from a straightforward association of the thickness anomalies around the YWS with the climatic impacts of the 1815 CE Tambora eruption, climate should still be considered as a potentially important factor due to the noticeable climate anomaly around the YWS found for each location. For Etoliko (Greece), there was a change in NH summer precipitation that reached almost 150% of the long-term average, whereas for all the remaining lakes, there was either a summer or winter temperature change of at least 1.5 °C (Fig. 2).

Although records from the third category are more likely to contain the imprint of the YWS than those from the first two categories, non-climatic drivers of VT anomalies should also be considered. For instance, in lakes with well-documented human impact across the YWS, such as Żabińskie in Poland (Żarczynski et al., 2019), an anthropogenic trigger potentially can dominate VT variations. Additionally, random processes unrelated to environmental disturbances, such as sediment redeposition due to slumping, could explain VT anomalies (Apolinarska et al., 2020). Therefore, without additional evidence supporting associations of VT anomalies in this category with climate perturbation, we consider the YWS imprint to be questionable.

4.2.4. YWS imprint likely

This last category comprises five records, for which we found anomalously thin or thick layers at 1816 ± 7 CE, along with noticeable climate anomalies at the sites of the records. Additionally, for a record to be included in this category, the thickness anomalies had to correspond to the climate anomaly, with which it revealed the strongest association. Two records, Kusai - dark layer and Kuninkaisenlampi - light layer, were included in this category conditionally and require some caution.

A positive anomaly in the Kusai - dark layer record was identified as possibly related to the YWS based on the results of a climate modeling study by Wegmann et al. (2014) that suggested, this location experienced a positive summer wind anomaly during 1816 CE. We suggest caution in this case because the results of climate modeling reveal high spatial variability of anomalies around the location of Lake Kusai. Additionally, the wind anomalies modelled lack independent confirmation.

In the case of Kuninkaisenlampi - light layer, caution is required because the thickness is assumed to respond mostly to hydrological extremes, for which we have no independent proxy. The record was included in the fourth category because Saarni et al. (2016) suggested that hydrological extremes are inversely related to winter temperatures. Since winter temperature for the location of Lake Kuninkaisenlampi was higher by ~1.5 °C compared to the long-term average, we consider it likely that negative thickness anomalies correspond to this warming. For the Kuninkaisenlampi - light layer record, an additional factor is complicating the association of the VT anomaly with the climate fluctuation following the 1815 CE Tambora eruption, which is the presence of several consecutive VT anomalies for the period 1816 ± 7 CE (Fig. 6). One possible explanation for the occurrence of consecutive anomalies is related to the hydrological memory of the catchment, which could allow a climatic anomaly to influence the hydrological behavior of a catchment for several years (de Lavenne et al., 2022). However, it remains unclear whether this or other factors caused these multiple anomalies.

For the remaining lakes in the fourth category, the relevant climate anomaly is derived from the output of EKF400v2. Because all these investigated lake records are located in or near Europe, where abundant observational information is available (Valler et al., 2022), a high confidence in the reconstructed climate anomaly is expected. The thickness

anomaly that likely corresponds to the YWS in the Holzmaar varve record (Germany) has the largest scaled magnitude over the entire period considered (Fig. 6). Although it is not conclusive from correlation with instrumental data, which season drives VT the most (Zolitschka, 1998), given the pronounced NH summer cooling (>2 °C; Fig. 2) and the inverse relationship with temperature (Fig. 3), we assume that the warm season cooling forced the exceptional thickness of the varve, while the reconstructed winter warming had no clear impact on VT for this site.

For the Nar Gölü - light layer record, there are three thickness anomalies in the period 1816 ± 7 CE: two negative anomalies, which are both of a small-scaled magnitude, and one positive anomaly, which is large (Fig. 6). Light layer thickness of the Nar Gölü record is positively related to spring precipitation (Fig. 3). Therefore, it is most likely that the large, positive thickness anomaly resulted from excessive spring precipitation (>120% of the long-term mean according to EKF400v2; data not shown) followed by an exceptionally wet summer (precipitation exceeded 200% of the long-term mean; Fig. 2). If this association of the positive anomaly with the YWS is correct, then the origin of the negative anomalies must be explained by other factors.

The Oeschinen varve record revealed two anomalies at 1816 ± 7 CE: a larger and positive and a smaller and negative (Fig. 6). We assume that it is the positive thickness anomaly that recorded the climatic effect of the 1815 CE Tambora eruption. The most prominent climate anomaly during the YWS reported for the location of Oeschinen is a NH summer cooling that exceeded 2.5 °C (Fig. 2). However, as the varve thickness is primarily related to precipitation (Fig. 3), it is more likely that the YWS imprint is associated with the precipitation anomaly, which reached 120% of the long-term average (Fig. 2). It is well documented that the NH summer of 1816 CE was exceptionally wet in Switzerland, even if it was the number of days with precipitation rather than the total precipitation sum that differed markedly from average conditions (Brönnimann and Krämer, 2016).

5. Conclusions

In this study, we examined 38 VT records covering the period from 1766 to 1866 CE to investigate imprints of the prominent climate anomaly following the 1815 CE Tambora eruption, known as the 1816 'Year Without a Summer' (YWS). We hypothesize that thickness anomalies correspond to the YWS in many VT records because it was one of the most prominent climatic events of recent centuries (Sigl et al., 2015). Moreover, VT is a sensitive climate recorder. However, with the statistical methods applied, we document that the imprint of the YWS is missing in most cases.

There are two main reasons for only a limited number of records containing the YWS signal. First, although the climate anomaly was prominent on a global scale, many of the studied sites experienced only limited shifts in temperature and precipitation. Thus, the climate forcing affecting lake sedimentation was likely too weak to cause distinct VT anomalies. Only in a few cases climate forcing was noticeable. However, either the season revealing the anomaly or the climate variable that noticeably departed from the long-term mean were not the primary drivers of VT as recognized in the original studies. The lack of thickness anomalies in these cases shows that VT is a poor recorder of even prominent climate anomalies if the climatic conditions relevant to varve formation remain stable at a given site. Therefore, globally correlated varve thickness anomalies should not be expected from climate impacts even of the most violent Late Holocene volcanic eruption.

Nevertheless, the likely presence of an imprint of the YWS in five time series corroborates the ability of VT to record annual climate anomalies. Therefore, they should be considered, among other drivers, as a likely factor behind event-like changes in varve thickness records.

We argue that future multi-proxy studies of lake sediments should consider the examination of a likely imprint of the YWS. This will enable more detailed interpretations of lake ecosystem responses associated with such events. However, and perhaps the most challenging task for future studies focusing on volcanic imprints on lake sediment archives is finding an independent proxy for a volcanic event that would allow a more direct association of changes in sediment records with volcanic events such as the YWS. In the absence of tephra particles and/or advanced chronological methods to improve the dating of varve sediments from the distant past, these records will inevitably be limited by chronological uncertainties. This makes a precise correlation of short-term climatic events with multi-centennial or longer timescales challenging, if not unfeasible.

CRediT authorship contribution statement

Krzysztof Pleskot: Conceptualization, Data curation, Formal analysis, Funding acquisition, Visualization, Writing – original draft. **Bernd Zolitschka:** Conceptualization, Supervision, Writing – review & editing.

Declaration of generative AI and AI-assisted technologies in the writing process

During the preparation of this work the authors used ChatGPT in order to improve readability and language. After using this tool, the authors reviewed and edited the content as needed and take full responsibility for the content of the publication.

Declaration of competing interest

The authors declare that they have no known competing financial interests or personal relationships that could have appeared to influence the work reported in this paper.

Acknowledgements

We thank Francois Lapointe and an anonymous reviewer for their thoughtful suggestions, which improved the quality of this work. The study was financed through a grant from the Polish National Agency for Academic Exchange NAWA, contract no. BPN/BEK/2023/1/00024/U/00001. We would like to thank all the authors who uploaded their data to public repositories, making this study possible. We are also thankful to those who shared their data with us, including Neil Roberts, Maurycy Żarczyński, Xingqi Liu, Saija Saarni, and Christian Bigler.

Appendix A. Supplementary data

Supplementary data to this article can be found online at https://doi.org/10.1016/j.quascirev.2024.109085.

Data availability

The paleo-reanalysis dataset EKF400v2 can be obtained from https://www.wdc-climate.de/ui/entry?acronym=EKF400_ens_mem_Mean_v2.0 following registration. The majority of the varve thickness data is available from VARDA (https://varve.gfz-potsdam.de/), WDS-Paleo (https://www.ncei.noaa.gov/access/paleo-search/), PANGAEA (https://pangaea.de/), the Geological Society of America (GSA) Data Repository (https://www.geosociety.org/GSA/GSA/Pubs/data-repository.aspx) and the Arctic Data Center (https://arcticdata.io/) as listed in Table 1. The remaining records and the code to reproduce the analyses are available at https://github.com/krzypl/ms_varvol_db.

References

Amann, B., Lamoureux, S.F., Boreux, M.P., 2017. Winter temperature conditions (1670–2010) reconstructed from varved sediments, western Canadian High Arctic. Quat. Sci. Rev. 172, 1–14. https://doi.org/10.1016/j.quascirev.2017.07.013.

Amann, B., Szidat, S., Grosjean, M., 2015. A millennial-long record of warm season precipitation and flood frequency for the North-western Alps inferred from varved

lake sediments: implications for the future. Quat. Sci. Rev. 115, 89–100. https://doi.org/10.1016/j.quascirev.2015.03.002.
Apolinarska, K., Pleskot, K., Pełechata, A., Migdałek, M., Siepak, M., Pełechaty, M., 2020. The recent deposition of laminated sediments in highly eutrophic Lake Kierskie, western Poland: 1 year pilot study of limnological monitoring and sediment traps. J. Paleolimnol. 63, 283–304. https://doi.org/10.1007/s10933-020-00116-2.
Arnqvist, P., Bigler, C., Renberg, I., Sjöstedt de Luna, S., 2016. Functional clustering of varved lake sediment to reconstruct past seasonal climate. Environ. Ecol. Stat. 23, 513–529. https://doi.org/10.1007/s10651-016-0351-1.
Besonen, M.R., Bradley, R.S., Mudelsee, M., Abbott, M.B., Francus, P., 2008. A 1,000-year, annually-resolved record of hurricane activity from Boston, Massachusetts. Geophys. Res. Lett. 35, L14705. https://doi.org/10.1029/2008GL033950.
Bird, B.W., Abbott, M.B., Finney, B.P., Kutchko, B., 2009. A 2000 year varve-based climate record from the central Brooks Range, Alaska. J. Paleolimnol. 41, 25–41. https://doi.org/10.1007/s10933-008-9262-y.
Blass, A., Grosjean, M., Troxler, A., Sturm, M., 2007. How stable are twentieth-century calibration models? A high-resolution summer temperature reconstruction for the eastern Swiss Alps back to AD 1580 derived from proglacial varved sediments. Holocene 17, 51–63. https://doi.org/10.1177/0959683607073278.
Boes, E., Van Daele, M., Moernaut, J., Schmidt, S., Jensen, B.J.L., Praet, N., Kaufman, D., Haeussler, P., Loso, M.G., De Batist, M., 2017. Varve formation during the past three centuries in three large proglacial lakes in south-central Alaska. GSA Bull. 130, 757–774. https://doi.org/10.1130/B31792.1.
Brönnimann, S., Krämer, D., 2016. Tambora and the "year without a summer" of 1816. A perspective on Earth and human systems science. G90. Geographica Bernensia G90, 48. https://doi.org/10.4480/GB2016.G90.01.
Cook, T.L., Bradley, R.S., Stoner, J.S., Francus, P., 2009. Five thousand years of sediment transfer in a high arctic watershed recorded in annually laminated sediments from Lower Murray Lake, Ellesmere Island, Nunavut, Canada. J. Paleolimnol. 41, 77–94. https://doi.org/10.1007/s10933-008-9252-0.
Cooper, C.L., Swindles, G.T., Savov, I.P., Schmidt, A., Bacon, K.L., 2018. Evaluating the relationship between climate change and volcanism. Earth Sci. Rev. 177, 238–247. https://doi.org/10.1016/j.earscirev.2017.11.009.
Courtney Mustaphi, C.J., Gajewski, K., 2013. Holocene sediments from a coastal lake on northern Devon Island, Nunavut, Canada. Can. J. Earth Sci. 50, 564–575. https://doi.org/10.1139/cjes-2012-0143.
Cuven, S., Francus, P., Lamoureux, S., 2011. Mid to late Holocene hydroclimatic and geochemical records from the varved sediments of East Lake, Cape Bounty, Canadian High Arctic. Quat. Sci. Rev. 30, 2651–2665. https://doi.org/10.1016/j.quascirev.2011.05.019.
de Lavenne, A., Andréassian, V., Crochemore, L., Lindström, G., Arheimer, B., 2022. Quantifying multi-year hydrological memory with catchment forgetting curves. Hydrol. Earth Syst. Sci. 26, 2715–2732. https://doi.org/10.5194/hess-26-2715-2022.
Dean, W.E., Megard, R.O., 1993. Environment of deposition of CaCO3 in Elk Lake, Minnesota. In: Bradbury, J.P., Dean, W.E. (Eds.), Elk Lake, Minnesota: Evidence for Rapid Climate Change in the North-Central United States, vol. 276. Geological Society of America, pp. 97–113. https://doi.org/10.1130/SPE276-p97.
Diedrich, K.E., Loso, M.G., 2012. Transient impacts of Little Ice Age glacier expansion on sedimentation processes at glacier-dammed Iceberg Lake, southcentral Alaska. J. Paleolimnol. 48, 115–132. https://doi.org/10.1007/s10933-012-9614-5.
Elbert, J., Jacques-Coper, M., Van Daele, M., Urrutia, R., Grosjean, M., 2015. A 600 years warm-season temperature record from varved sediments of Lago Plomo, Northern Patagonia, Chile (47°S). Quat. Int. 377, 28–37. https://doi.org/10.1016/j.quaint.2015.01.004.
Emile-Geay, J., McKay, N.P., Kaufman, D.S., von Gunten, L., Wang, J., Anchukaitis, K.J., Abram, N.J., Addison, J.A., Curran, M.A.J., Evans, M.N., Henley, B.J., Hao, Z., Martrat, B., McGregor, H.V., Neukom, R., Pederson, G.T., Stenni, B., Thirumalai, K., Werner, J.P., Xu, C., Divine, D.V., Dixon, B.C., Gergis, J., Mundo, I.A., Nakatsuka, T., Phipps, S.J., Routson, C.C., Steig, E.J., Tierney, J.E., Tyler, J.J., Allen, K.J., Bertler, N.A.N., Björklund, J., Chase, B.M., Chen, M.-T., Cook, E., de Jong, R., DeLong, K.L., Dixon, D.A., Ekaykin, A.A., Ersek, V., Filipsson, H.L., Francus, P., Freund, M.B., Frezzotti, M., Gaire, N.P., Gajewski, K., Ge, Q., Goosse, H., Gornostaeva, A., Grosjean, M., Horiuchi, K., Hormes, A., Husum, K., Isaksson, E., Kandasamy, S., Kawamura, K., Kilbourne, K.H., Koç, N., Leduc, G., Linderholm, H. W., Lorrey, A.M., Mikhalenko, V., Mortyn, P.G., Motoyama, H., Moy, A.D., Mulvaney, R., Munz, P.M., Nash, D.J., Oerter, H., Opel, T., Orsi, A.J., Ovchinnikov, D.V., Porter, T.J., Roop, H.A., Saenger, C., Sano, M., Sauchyn, D., Saunders, K.M., Seidenkrantz, M.-S., Severi, M., Shao, X., Sicre, M.-A., Sigl, M., Sinclair, K., St. George, S., St. Jacques, J.-M., Thamban, M., Kuwar Thapa, U., Thomas, E.R., Turney, C., Uemura, R., Viau, A.E., Vladimirova, D.O., Wahl, E.R., White, J.W.C., Yu, Z., Zinke, J., PAGES2k Consortium, 2017. A global multiproxy database for temperature reconstructions of the Common Era. Sci. Data 4, 170088. https://doi.org/10.1038/sdata.2017.88.
Felden, J., Möller, L., Schindler, U., Huber, R., Schumacher, S., Koppe, R., Diepenbroek, M., Glöckner, F.O., 2023. PANGAEA - data publisher for Earth & environmental science. Sci. Data 10, 347. https://doi.org/10.1038/s41597-023-02269-x.
Fischer, E.M., Luterbacher, J., Zorita, E., Tett, S.F.B., Casty, C., Wanner, H., 2007. European climate response to tropical volcanic eruptions over the last half millennium. Geophys. Res. Lett. 34, 2006GL027992. https://doi.org/10.1029/2006GL027992.
Francus, P., Bradley, R.S., Abbott, M.B., Patridge, W., Keimig, F., 2002. Paleoclimate studies of minerogenic sediments using annually resolved textural parameters. Geophys. Res. Lett. 29. https://doi.org/10.1029/2002GL015082, 59-1-59–4.
Fritz, S.C., 2007. Deciphering climatic history from lake sediments. J. Paleolimnol. 39, 5–16. https://doi.org/10.1007/s10933-007-9134-x.
Gross, W., Morrill, C., Wahl, E., 2018. New advances at NOAA's World data Service for Paleoclimatology – promoting the FAIR principles. Past Glob. Change Mag 26. https://doi.org/10.22498/pages.26.2.58, 58–58.
Haltia-Hovi, E., Saarinen, T., Kukkonen, M., 2007. A 2000-year record of solar forcing on varved lake sediment in eastern Finland. Quat. Sci. Rev. 26, 678–689. https://doi.org/10.1016/j.quascirev.2006.11.005.
Hughen, K.A., 2009. NOAA/WDS Paleoclimatology - Ogac Lake, Baffin Island 2,000 Year varve thickness data. https://doi.org/10.25921/AQEX-W486.
Hughen, K.A., Overpeck, J.T., Anderson, R.F., 2000. Recent warming in a 500-year palaeotemperature record from varved sediments, upper Soper Lake, Baffin Island, Canada. Holocene 10, 9–19. https://doi.org/10.1191/095968300676746202.
Iles, C.E., Hegerl, G.C., Schurer, A.P., Zhang, X., 2013. The effect of volcanic eruptions on global precipitation. J. Geophys. Res. Atmos. 118, 8770–8786. https://doi.org/10.1002/jgrd.50678.
Kaufman, D.S., Broadman, E., 2023. Revisiting the Holocene global temperature conundrum. Nature 614, 425–435. https://doi.org/10.1038/s41586-022-05536-w.
Koutsodendris, A., Brauer, A., Reed, J.M., Plessen, B., Friedrich, O., Hennrich, B., Zacharias, I., Pross, J., 2017. Climate variability in SE Europe since 1450 AD based on a varved sediment record from Etoliko Lagoon (Western Greece). Quat. Sci. Rev. 159, 63–76. https://doi.org/10.1016/j.quascirev.2017.01.010.
Lamoureux, S.F., Bradley, R.S., 1996. A late Holocene varved sediment record of environmental change from northern Ellesmere Island, Canada. J. Paleolimnol. 16, 239–255. https://doi.org/10.1007/BF00176939.
Lapointe, F., Francus, P., Lamoureux, S.F., Vuille, M., Jenny, J.-P., Bradley, R.S., Massa, C., 2017. Influence of North Pacific decadal variability on the western Canadian Arctic over the past 700 years. Clim. Past 13, 411–420. https://doi.org/10.5194/cp-13-411-2017.
Lapointe, F., Retelle, M., Bradley, R.S., Farnsworth, W.R., Støren, E., Cook, T., Rosario, J., 2023. Multi-proxy evidence of unprecedented hydroclimatic change in a high Arctic proglacial lake: Linnévatnet, Svalbard. Arctic Antarct. Alpine Res. 55, 2223403. https://doi.org/10.1080/15230430.2023.2223403.
Larsen, D.J., Miller, G.H., Geirsdóttir, Á., Thordarson, T., 2011. A 3000-year varved record of glacier activity and climate change from the proglacial lake Hvítárvatn, Iceland. Quat. Sci. Rev. 30, 2715–2731. https://doi.org/10.1016/j.quascirev.2011.05.026.
Li, J., Xie, S.-P., Cook, E.R., Morales, M.S., Christie, D.A., Johnson, N.C., Chen, F., D'Arrigo, R., Fowler, A.M., Gou, X., Fang, K., 2013. El Niño modulations over the past seven centuries. Nat. Clim. Change 3, 822–826. https://doi.org/10.1038/nclimate1936.
Loso, M.G., 2009. Summer temperatures during the Medieval Warm Period and Little Ice Age inferred from varved proglacial lake sediments in southern Alaska. J. Paleolimnol. 41, 117–128. https://doi.org/10.1007/s10933-008-9264-9.
Luterbacher, J., Pfister, C., 2015. The year without a summer. Nat. Geosci. 8, 246–248. https://doi.org/10.1038/ngeo2404.
Moore, J.J., Hughen, K.A., Miller, G.H., Overpeck, J.T., 2001. Little Ice Age recorded in summer temperature reconstruction from vared sediments of Donard Lake, Baffin Island, Canada. J. Paleolimnol. 25, 503–517. https://doi.org/10.1023/A:1011181301514.
Mudelsee, M., 2014. Climate time series analysis: classical statistical and bootstrap methods, 2. Atmospheric and Oceanographic Sciences Library. Springer, Cham Heidelberg, p. 454.
Neukom, R., Barboza, L.A., Erb, M.P., Shi, F., Emile-Geay, J., Evans, M.N., Franke, J., Kaufman, D.S., Lücke, L., Rehfeld, K., Schurer, A., Zhu, F., Brönnimann, S., Hakim, G.J., Henley, B.J., Ljungqvist, F.C., McKay, N., Valler, V., von Gunten, L., PAGES 2k Consortium, 2019. Consistent multidecadal variability in global temperature reconstructions and simulations over the Common Era. Nat. Geosci. 12, 643–649. https://doi.org/10.1038/s41561-019-0400-0.
Ojala, A.E.K., Alenius, T., 2005. 10,000 years of interannual sedimentation recorded in the Lake Nautajärvi (Finland) clastic–organic varves. Palaeogeogr. Palaeoclimatol. Palaeoecol. 219, 285–302. https://doi.org/10.1016/j.palaeo.2005.01.002.
Ojala, A.E.K., Francus, P., Zolitschka, B., Besonen, M., Lamoureux, S.F., 2012. Characteristics of sedimentary varve chronologies – a review. Quat. Sci. Rev. 43, 45–60. https://doi.org/10.1016/j.quascirev.2012.04.006.
Olonscheck, D., Schurer, A.P., Lücke, L., Hegerl, G.C., 2021. Large-scale emergence of regional changes in year-to-year temperature variability by the end of the 21st century. Nat. Commun. 12, 7237. https://doi.org/10.1038/s41467-021-27515-x.
Ortega, P., Lehner, F., Swingedouw, D., Masson-Delmotte, V., Raible, C.C., Casado, M., Yiou, P., 2015. A model-tested North Atlantic Oscillation reconstruction for the past millennium. Nature 523, 71–74. https://doi.org/10.1038/nature14518.
Raible, C.C., Brönnimann, S., Auchmann, R., Brohan, P., Frölicher, T.L., Graf, H., Jones, P., Luterbacher, J., Muthers, S., Neukom, R., Robock, A., Self, S., Sudrajat, A., Timmreck, C., Wegmann, M., 2016. Tambora 1815 as a test case for high impact volcanic eruptions: Earth system effects. WIREs Clim. Change 7, 569–589. https://doi.org/10.1002/wcc.407.
Ramisch, A., Brauser, A., Dorn, M., Blanchet, C., Brademann, B., Köppl, M., Mingram, J., Neugebauer, I., Nowaczyk, N., Ott, F., Pinkerneil, S., Plessen, B., Schwab, M.J., Tjallingii, R., Brauer, A., 2020. VARDA (VARved sediments DAtabase) – providing and connecting proxy data from annually laminated lake sediments. Earth Syst. Sci. Data 12, 2311–2332. https://doi.org/10.5194/essd-12-2311-2020.
Roberts, N., Allcock, S.L., Barnett, H., Mather, A., Eastwood, W.J., Jones, M., Primmer, N., Yiğitbaşıoğlu, H., Vannière, B., 2019. Cause-and-effect in Mediterranean erosion: the role of humans and climate upon Holocene sediment flux into a central Anatolian lake catchment. Geomorphology, Human Geomorphological

Interactions and the Legacy of Karl Butzer 331, 36–48. https://doi.org/10.1016/j.geomorph.2018.11.016.
Saarni, S., Muschitiello, F., Weege, S., Brauer, A., Saarinen, T., 2016. A late Holocene record of solar-forced atmospheric blocking variability over Northern Europe inferred from varved lake sediments of Lake Kuninkaisenlampi. Quat. Sci. Rev. 154, 100–110. https://doi.org/10.1016/j.quascirev.2016.10.019.
Schiefer, E., Menounos, B., Slaymaker, O., 2007. Extreme sediment delivery events recorded in the contemporary sediment record of a montane lake, southern Coast Mountains, British Columbia. Can. J. Earth Sci. 43, 1777–1790. https://doi.org/10.1139/e06-056.
Sigl, M., Winstrup, M., McConnell, J.R., Welten, K.C., Plunkett, G., Ludlow, F., Buntgen, U., Caffee, M., Chellman, N., Dahl-Jensen, D., Fischer, H., Kipfstuhl, S., Kostick, C., Maselli, O.J., Mekhaldi, F., Mulvaney, R., Muscheler, R., Pasteris, D.R., Pilcher, J.R., Salzer, M., Schupbach, S., Steffensen, J.P., Vinther, B.M., Woodruff, T. E., 2015. Timing and climate forcing of volcanic eruptions for the past 2,500 years. Nature 523, 543–549. https://doi.org/10.1038/nature14565.
Thomas, E.K., Briner, J.P., 2009. Climate of the past millennium inferred from varved proglacial lake sediments on northeast Baffin Island, Arctic Canada. J. Paleolimnol. 41, 209–224. https://doi.org/10.1007/s10933-008-9258-7.
Thomas, E.K., McGrane, S., Briner, J.P., Huang, Y., 2012. Leaf wax δ2H and varve-thickness climate proxies from proglacial lake sediments, Baffin Island, Arctic Canada. J. Paleolimnol. 48, 193–207. https://doi.org/10.1007/s10933-012-9584-7.
Tierney, J.E., Poulsen, C.J., Montañez, I.P., Bhattacharya, T., Feng, R., Ford, H.L., Hönisch, B., Inglis, G.N., Petersen, S.V., Sagoo, N., Tabor, C.R., Thirumalai, K., Zhu, J., Burls, N.J., Foster, G.L., Goddéris, Y., Huber, B.T., Ivany, L.C., Kirtland Turner, S., Lunt, D.J., McElwain, J.C., Mills, B.J.W., Otto-Bliesner, B.L., Ridgwell, A., Zhang, Y.G., 2020. Past climates inform our future. Science 370, eaay3701. https://doi.org/10.1126/science.aay3701.
Trigo, R.M., Vaquero, J.M., Alcoforado, M., Barriendos, M., Taborda, J., García-Herrera, R., Luterbacher, J., 2009. Iberia in 1816, the year without a summer. Int. J. Climatol. 29, 99–115. https://doi.org/10.1002/joc.1693.
Valler, V., Franke, J., Brugnara, Y., Brönnimann, S., 2022. An updated global atmospheric paleo-reanalysis covering the last 400 years. Geosci. Data J 9, 89–107. https://doi.org/10.1002/gdj3.121.
Vegas-Vilarrúbia, T., Corella, J.P., Sigró, J., Rull, V., Dorado-Liñan, I., Valero-Garcés, B., Gutiérrez-Merino, E., 2022. Regional precipitation trends since 1500 CE reconstructed from calcite sublayers of a varved Mediterranean lake record (Central Pyrenees). Sci. Total Environ. 826, 153773. https://doi.org/10.1016/j.scitotenv.2022.153773.
Wang, F., Arseneault, D., Boucher, É., Gennaretti, F., Lapointe, F., Yu, S., Francus, P., 2023. Volcanic imprints in last-millennium land summer temperatures in the Circum–North Atlantic Area. J. Clim. 36, 5923–5939. https://doi.org/10.1175/JCLI-D-23-0107.1.
Wegmann, M., Brönnimann, S., Bhend, J., Franke, J., Folini, D., Wild, M., Luterbacher, J., 2014. Volcanic influence on European summer precipitation through monsoons: possible cause for “years without summer.”. J. Clim. 27, 3683–3691. https://doi.org/10.1175/JCLI-D-13-00524.1.
Wolff, C., Haug, G.H., Timmermann, A., Damsté, J.S.S., Brauer, A., Sigman, D.M., Cane, M.A., Verschuren, D., 2011. Reduced interannual rainfall variability in East Africa during the last Ice Age. Science 333, 743–747. https://doi.org/10.1126/science.1203724.
Żarczynski, M., Wacnik, A., Tylmann, W., 2019. Tracing lake mixing and oxygenation regime using the Fe/Mn ratio in varved sediments: 2000year-long record of human-induced changes from Lake Żabińskie (NE Poland). Sci. Total Environ. 657, 585–596. https://doi.org/10.1016/j.scitotenv.2018.12.078.
Zhang, Q., Liu, X., Feng, S., 2022. Factors influencing the seasonal flux of the varved sediments of Kusai Lake on the northern Tibetan Plateau during the last ~2280 years. Front. Earth Sci. 9. https://doi.org/10.3389/feart.2021.823258.
Zheng, Z., Yang, Y., 1998. Cross-validation and median criterion. Stat. Sin. 8, 907–921. https://www.jstor.org/stable/24306470.
Zolitschka, B., 1998. Paläoklimatische Bedeutung Laminierter Sedimente: Holzmaar (Eifel, Deutschland), Lake C2 (Nordwest-Territorien, Kanada) und Lago Grande di Monticchio (Basilicata, Italien), Relief, Boden, Paläoklima. Borntraeger, Berlin, p. 176.
Zolitschka, B., 1996. High resolution lacustrine sediments and their potential for Palaeoclimatic reconstruction. In: Jones, P.D., Bradley, R.S., Jouzel, J. (Eds.), Climatic Variations and Forcing Mechanisms of the Last 2000 Years. Springer Berlin Heidelberg, Berlin, Heidelberg, pp. 453–478. https://doi.org/10.1007/978-3-642-61113-1_21.
Zolitschka, B., Francus, P., Ojala, A.E.K., Schimmelmann, A., 2015. Varves in lake sediments – a review. Quat. Sci. Rev. 117, 1–41. https://doi.org/10.1016/j.quascirev.2015.03.019.